JACS
JOURNAL OF THE AMERICAN CHEMICAL SOCIETY
Communication
pubs.acs.org/JACS

Boosting the Sensitivity of Ligand–Protein Screening by NMR of Long-Lived States

Nicola Salvi,[†] Roberto Buratto,[†] Aurélien Bornet,*[,†] Simone Ulzega,[†,⊥] Inmaculada Rentero Rebollo,[†] Alessandro Angelini,[†,#] Christian Heinis,[†] and Geoffrey Bodenhausen[†,‡,§,∥]

[†]Institut des Sciences et Ingénierie Chimiques, Ecole Polytechnique Fédérale de Lausanne, 1015 Lausanne, Switzerland
[‡]Département de Chimie, Ecole Normale Supérieure, 75231 Paris Cedex 05, France
[§]UMR 7203, CNRS/UPMC/ENS, Paris, France
[∥]Université de Pierre-et-Marie Curie, Paris, France

Supporting Information

ABSTRACT: A new NMR method for the study of ligand–protein interactions exploits the unusual lifetimes of long-lived states (LLSs). The new method provides better contrast between bound and free ligands and requires a protein–ligand ratio ca. 25 times lower than for established $T_{1\rho}$ methods, thus saving on costly proteins. The new LLS method was applied to the screening of inhibitors of urokinase-type plasminogen activator (uPA), which is a prototypical target of cancer research. With only 10 μM protein, a dissociation constant (K_D) of 180 ± 20 nM was determined for the strong ligand (inhibitor) UK-18, which can be compared with K_D = 157 ± 39 nM determined by the established surface plasmon resonance method.

A fundamental goal of pharmaceutical research and drug development is the quest for natural or synthetic molecules that interact strongly and specifically with a target biomolecule, promoting or inhibiting its activity. Screening can be carried out by, among others, enzyme-linked immunosorbent assay (ELISA),[1] fluorescence anisotropy,[2] isothermal titration calorimetry,[3] surface plasmon resonance,[4] and various NMR techniques.[5−7] The latter have proven to be particularly effective for the identification of new lead compounds that bind weakly and have fairly large dissociation constants K_D,

$$K_D = \frac{[P][L]}{[PL]} = \frac{k_{off}}{k_{on}} \quad (1)$$

where [P], [L], and [PL] are the concentrations of the free protein, free ligand (e.g., an inhibitor), and protein–ligand complex, respectively, while $k_{on} \gg k_{off}$ are the association and dissociation rates for the complex.[8] Established NMR methods[5−7] are useful over the range 100 μM < K_D < 10 mM, where traditional methods[1−4] often lack sensitivity. NMR spectroscopy can focus on either the proteins or the ligands by exploiting one of many possible probes,[9−13] such as chemical shifts, diffusion constants, relaxation rates, and magnetization transfer or saturation transfer rates. Some NMR methods can provide information with atomic resolution about the region (epitope) of the protein that is involved in binding.

Levitt and co-workers[14−16] discovered so-called long-lived states (LLSs), also known as singlet states (SSs), in two-spin systems. LLSs have the property that the magnetization decays with a time constant T_{LLS} that can be much longer than typical longitudinal spin–lattice relaxation time constants T_1. Here we exploited an LLS associated with a pair of protons attached to a weak ligand (without isotopic labeling) and determined its K_D by monitoring the change in the relaxation rate $R_{LLS} = 1/T_{LLS}$ when the weak ligand was added to a dilute (ca. 10 μM) protein solution (titration of the ligand). Competition experiments allowed K_D of stronger ligands to be determined by monitoring R_{LLS} of the weak ligand. Simulations showed that the proposed method benefits from *enhanced contrast* (i.e., a greater difference between R_{LLS} of the free and bound ligands) relative to analogous methods that exploit longitudinal relaxation rates $R_1 = 1/T_1$ or transverse relaxation rates $R_{1\rho}$ of spin-locked magnetization. Because of the enhanced contrast, this technique allows one to study strong interactions (in this work, 100 nM < K_D < 1 mM) using protein concentrations as small as 10 μM. Our method is illustrated by screening of inhibitors of a target for cancer therapy, the urokinase-type plasminogen activator (uPA),[17−19] a 52 kDa serine protease involved in tumor progression and metastasis formation.

If a ligand is in dynamic equilibrium between free and bound forms with an exchange rate constant $k_{ex} \approx k_{off}$ that is larger than the relevant chemical shift differences, all of the relaxation rates are averaged:[20,21]

$$\langle R_i \rangle = X^{bound} R_i^{bound} + X^{free} R_i^{free} \quad (2)$$

where i = 1 for longitudinal relaxation, i = 2 for transverse relaxation, $i = 1\rho$ for (preferably selective) $T_{1\rho}$ relaxation of spin-locked transverse magnetization, i = LLS for long-lived states, and i = LLC for long-lived coherences; R_i^{bound} and R_i^{free} are the relaxation rates of the bound and free ligands, respectively, and X^{bound} and X^{free} are the corresponding mole fractions. Hence,

$$\langle R_i \rangle = \frac{[P]_0}{K_D + [L]_0}(R_i^{bound} - R_i^{free}) + R_i^{free} \quad (3)$$

Received: April 5, 2012
Published: June 11, 2012

dx.doi.org/10.1021/ja303301w | J. Am. Chem. Soc. 2012, 134, 11076−11079

where $[P]_0$ and $[L]_0$ are the total protein and ligand concentrations, respectively. Equation 3 shows that large changes $\Delta R_i = R_i^{bound} - R_i^{free}$ induce large changes in $\langle R_i \rangle$. For each experiment i, we can define a dimensionless parameter to express its contrast for a given $[P]_0/[L]_0$ ratio:

$$C_i = \frac{\langle R_i \rangle - R_i^{free}}{\langle R_i \rangle} = \frac{T_i^{free} - \langle T_i \rangle}{T_i^{free}} \quad (4)$$

The smallest mole fraction X^{bound} that can be detected by a method i is proportional to its contrast C_i.

Both experimental results and numerical simulations show that the contrast is more favorable for R_{LLS} than for conventional longitudinal relaxation rates R_1 ($i = 1$) or for selective spin locking ($i = 1\rho$). In particular, we simulated the dipole−dipole contributions (the main relaxation pathways in solution-state NMR spectroscopy if chemical shift anisotropy can be neglected) to the R_1 and R_{LLS} relaxation rates of the free and bound tripeptide glycine-glycine-arginine (GGR) (See Materials and Methods and Figure 1). For the conventional longitudinal relaxation rates R_1, the dipole−dipole interactions between the protons of the ligand and those lining the binding site of uPA contribute roughly to 85% of the observed contrast [see Figure S4 in the Supporting Information (SI)].

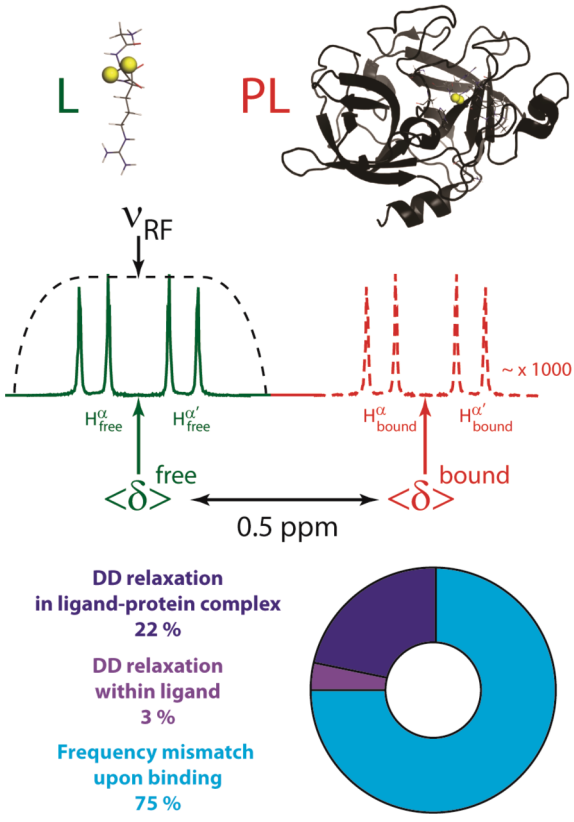

Figure 1. (top) Glycine-glycine-arginine (GGR) tripeptide and its complex with the protein uPA. (middle) Frequency jumps of the two H^{α} protons of the central glycine of GGR when it forms a complex with uPA. It is estimated that the two chemical shifts of the H^{α} protons jump by 0.5 ppm (or 200 Hz at 400 MHz) as the ligand goes from free (green solid line) to bound (red dashed line). The spectrum of the bound ligand cannot be observed directly because of the low concentration of the complex. (bottom) Relative contributions to the decay rate $R_{LLS} = 1/T_{LLS}$ of the long-lived state of the two H^{α} protons in the complex. The rf field used to sustain the LLS was monochromatic with an amplitude of $\nu_1 = 1$ kHz, well above the minimum required to mask the chemical shift difference $\delta(H^{\alpha}) - \delta(H^{\alpha'}) = 100$ Hz in the free ligand.

The chemical shifts of the two H^{α} protons of the central glycine residue in GGR in the free and bound forms were estimated by modeling (see Materials and Methods) to differ by ca. 0.5 ppm (200 Hz at 400 MHz in our experiments). Conventional longitudinal relaxation is not influenced by such a shift, but it has a dramatic effect on the lifetimes of the LLS.[22,23] Indeed, during the LLS relaxation period, a radiofrequency (rf) field must be used to mask the chemical shift difference between the two H^{α} protons involved in the LLS. This field is most efficient when the carrier frequency coincides precisely with the center between the shifts of the two H^{α} protons, as we chose for the free ligand. When the ligand is bound, there is a frequency mismatch due to the change in chemical shifts upon binding, and the LLS decays rapidly, so that its lifetime is reduced. Indeed, Figure 1 shows that ca. 75% of the decay rate of the LLS signal is due to the coherent effect of the frequency mismatch that occurs upon binding. This effect can be enhanced by using weaker rf fields or higher static fields. These coherent offset effects introduced by the rf field provide the rationale for the enhanced contrast of the LLS-based method.

Motional effects may further enhance the contrast. In particular, the rotational correlation time τ_C is much longer for the protein−ligand complex than for the free ligand. However, because the ligand may wiggle in the binding pocket, τ_C of the bound ligand may not be as long as the overall τ_C of the complex. Preliminary results (see Figure S5) showed that this contribution to the contrast should be significant, though less so than the coherent offset effect.

In general, relaxation rates offer a more direct and faster route to study ligand−protein interactions than diffusion-based methods.[24] The measurement of proton T_2's is impeded by echo modulations due to homonuclear J couplings.[25] Therefore, T_2-based methods are most straightforward for isolated heteronuclear spins[26] such as ^{19}F or require fitting of line shapes,[27] suppression of echo modulations,[28] or measurement of transverse relaxation times in the rotating frame ($T_{1\rho}$). Our LLS method does not suffer from any losses of versatility and sensitivity that the use of heteronuclei entails, nor does it suffer from the deleterious effects of inhomogeneous magnetic fields on line shapes.

Glycine residues in peptides contain two diastereotopic H^{α} protons, so it is straightforward to excite LLS in virtually any glycine-containing peptide.[29] It was shown by phage display[30] using a peptide library and consensus sequence analysis that peptides that bind to uPA must contain at least one arginine residue.[31] We therefore considered the GGR tripeptide, which turns out to be a weak ligand for uPA. In the free ligand L = GGR, the lifetime T_{LLS} of the two H^{α} protons in the central glycine was determined to be $T_{LLS}^{free} = 8.0 \pm 0.2$ s at 8 °C and 400 MHz. The ligand was then titrated over a range 0.5 mM < $[L]_0$ < 10 mM in the presence of $[P]_0 = 10$ μM uPA at 8 °C. The curve in Figure 2 was fitted to eq 3, yielding $K_D^{weak} = 220 \pm 10$ μM and $T_{LLS}^{bound} = 30 \pm 10$ ms (as expected, $T_{LLS}^{bound} \ll T_{LLS}^{free}$). In contrast, as shown in Figure 2, binding had virtually no effect on the longitudinal (spin−lattice) relaxation times T_1 of the same H^{α} protons. The contrast is clearly much better for T_{LLS} than for T_1. Parallel observations on trypsin show that the standard $T_{1\rho}$ method requires at least 25 times more protein to achieve the same contrast.

dx.doi.org/10.1021/ja303301w | J. Am. Chem. Soc. 2012, 134, 11076−11079

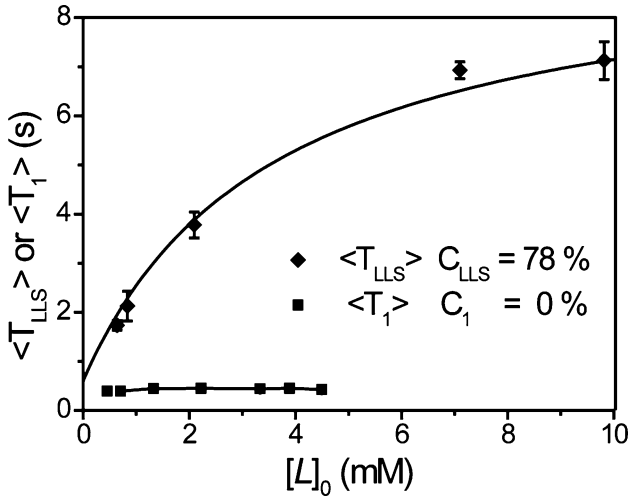

Figure 2. Lifetimes T_{LLS} of the long-lived state associated with the two H^{α} protons of the central glycine residue of the weak ligand L = GGR (◆) and their conventional longitudinal relaxation times T_1 (■) in the presence of $[P]_0$ = 10 μM uPA as functions of $[L]_0$ at 8 °C and 400 MHz in D_2O. The curve shows a fit of the experimental data to eq 3.

When binding is strong, the lifetime of the ligand–protein complex may be too long on the NMR time scale, so the conditions for eq 2 are not fulfilled and the rates are not properly averaged. In such cases, the LLS method can nevertheless be used by performing competition experiments in which a weak ligand such as GGR is titrated in the presence of a constant concentration of a stronger ligand that displaces the weaker ligand (Figure 3). Fitting to eq 5 with the known value of K_D^{weak} allows one to determine K_D^{strong}. In this fashion, we determined K_D^{strong} = 89 ± 20 μM for 4-aminobenzamidine, which has a better affinity than GGR but is not strong enough to inhibit uPA. Next we investigated the bicylic peptide ligand UK-18, which has a high affinity and specificity for uPA,[32] and we found this ligand to have K_D^{strong} = 180 ± 20 nM. The parameters extracted from the fits are compatible with previously published results obtained by Heinis and co-workers (K_D^{strong} = 157 ± 39 nM)[32] and Stubbs and co-workers (K_D^{strong} = 180 μM).[33] Thus, the LLS method allowed us to determine K_D^{strong} in a window that spans more than 3 orders of magnitude (180 nM < K_D^{strong} < 500 μM).

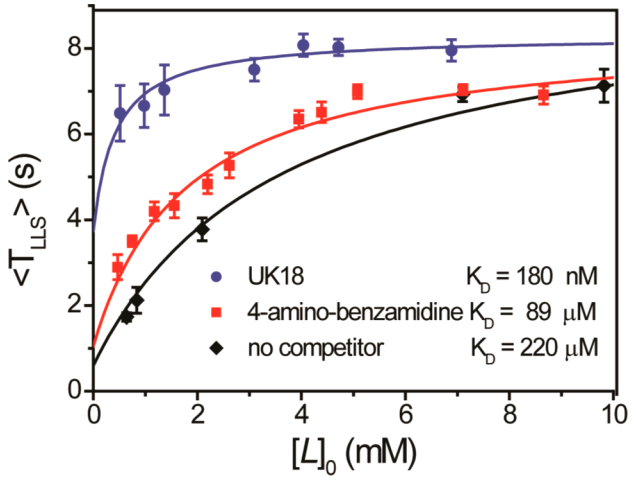

Figure 3. Lifetimes T_{LLS} of the long-lived state associated with the two H^{α} protons of the central glycine residue of the weak tripeptide ligand L = GGR in the presence of $[P]_0$ = 10 μM uPA as a function of the concentration $[L^{weak}]_0$ at 8 °C in D_2O: (◆) in the absence of any competing ligands; (■) in the presence of $[L^{strong}]_0$ = 12 μM 4-aminobenzamidine, which has a medium affinity; and (●) in the presence of $[L^{strong}]_0$ = 12 μm UK-18, which has a very high affinity. All data were obtained under the same conditions as in Figure 1. Experimental data obtained in the absence of competitors were fitted to eq 3. The K_D^{weak} and T_{LLS}^{bound} values extracted from this fit were used as fixed parameters when the titration curves measured in the presence of the additional stronger ligands were fitted to eq 5 describing the effects of competitors.

Long-lived states can thus be used to determine dissociation constants K_D of protein–ligand interactions with dramatically increased contrast. In comparison with $T_{1\rho}$-based methods, the optimal protein/ligand ratio $[P]_0/[L]_0$ can be reduced by a factor of ca. 25. On the one hand, the protein concentration needed to achieve the same relative change between averaged and free relaxation rates can be greatly reduced. On the other hand, if the protein concentration is kept constant, the amount of ligand can be increased, reducing the experimental time. Finally, for the same protein/ligand ratio, the LLS method offers better sensitivity. LLSs can readily be sustained in virtually any two-spin system. For instance, the use of peptides containing glycines offers a broad range of inexpensive weak ligands that lend themselves to competitive binding studies. LLSs can be used for screening a *library of compounds* for drug discovery: a spectrum of a weak "test" ligand can be acquired with a fixed interval where the LLS is sustained. When the weak test ligand is displaced by a stronger ligand, the signal of the test ligand is dramatically amplified. The combination of the LLS method with competitive binding methods gives access to a broad range of dissociation constants spanning nearly 5 orders of magnitude.

Materials and Methods.

1. Samples. uPA was prepared as explained elsewhere.[32] The synthetic GGR tripeptide (>75% purity from GenScript) was titrated over a range 0.5 mM < $[L]_0$ < 25 mM into (a) a solution containing 10 μM uPA in HEPES-buffered saline (5 mM HEPES buffer, pH 7.0, 10 mM NaCl) (solution 1); (b) a solution containing 10 μM uPA in the presence of $[L^{strong}]_0$ = 12 μM 4-aminobenzamidine (98% purity, Sigma-Aldrich) (solution 2); or (c) a solution containing 10 μM uPA in the presence of $[L^{strong}]_0$ = 12 μM UK-18, produced as explained elsewhere[32] (solution 3). An accurate amount (5 mM) of *tert*-butyl alcohol (99.5%, Sigma-Aldrich) was added as internal concentration standard. The concentrations of the stock solutions of both uPA and UK-18 were measured with a NanoDrop instrument (ThermoScientific).

2. Experimental procedures. During the titrations, 2 μL aliquots of a 70 mM GGR solution were added to 300 μL of solutions 1, 2, and 3. Lifetimes T_{LLS} were obtained by monoexponential fitting of signal intensities observed with the LLS pulse sequence[34] (see the SI) using 10 different sustaining delays 0.5 s < τ_{LLS} < 5T_{LLS}. All NMR measurements were performed on a 400 MHz (9.4 T) spectrometer in D_2O at 8 °C to avoid denaturation of the protein.

3. Fitting of titration curves. The experimental data obtained in the absence of any competitor were fitted to eq 3. In the presence of a competing ligand, the results were fitted to

dx.doi.org/10.1021/ja303301w | J. Am. Chem. Soc. 2012, 134, 11076–11079

$$\langle R_{LLS}^{weak} \rangle = \frac{[P]_{free}}{K_D + [L^{weak}]_0}(R_{LLS}^{weak,bound} - R_{LLS}^{weak,free}) + R_{LLS}^{weak,free} \quad (5)$$

where $\langle R_{LLS}^{weak} \rangle$, $R_{LLS}^{weak,bound}$, and $R_{LLS}^{weak,free}$ are the average, bound, and free LLS relaxation rates of the weak ligand, respectively, K_D^{weak} is its dissociation constant, and $[L^{weak}]_0$ is its total concentration. $[P]_{free}$ is the *remaining* free protein concentration available to bind to the weak ligand after the addition of a strong ligand:

$$[P]_{free} = [P]_0 - \frac{1}{2}\left\{[P]_0 + [L^{strong}]_0 + K_D^{strong} - \sqrt{([P]_0 + [L^{strong}]_0 + K_D^{strong})^2 - 4[P]_0[L^{strong}]_0}\right\} \quad (6)$$

where $[L^{strong}]_0$ is the total concentration of the competing strong ligand and K_D^{strong} is its dissociation constant (see sections 1−3 in the SI).

4. Structures of the ligand and the protein−ligand complex and chemical shift predictions. The structures of free GGR and the GGR−uPA complex in water were optimized using Gromacs 4.5.3[35] with the GROMOS 53a6 force field.[36] The chemical shifts for the free and bound ligands were then calculated using these structures as input for Camshift 1.35.[37]

■ ASSOCIATED CONTENT

Supporting Information

Derivation of eqs 3−5; details about the pulse sequence, modeling, chemical shift calculations; numerical simulations and estimates of the effect of the correlation time on the NMR relaxation rates of interest. This material is available free of charge via the Internet at http://pubs.acs.org.

■ AUTHOR INFORMATION

Corresponding Author

aurelien.bornet@epfl.ch

Present Addresses

[⊥]Bruker BioSpin AG, Industriestrasse 26, 8117 Fällanden, Switzerland.

[#]Massachusetts Institute of Technology, Building 76-261, 500 Main Street, Cambridge, MA 02139, USA.

Notes

The authors declare no competing financial interest.

■ ACKNOWLEDGMENTS

The authors gratefully acknowledge discussions with Dr. Claudio Dalvit, University of Neuchâtel. The work was supported by the Swiss National Science Foundation (FNRS), the Swiss Commission for Technology and Innovation (CTI), the EPFL, and the French CNRS.

■ REFERENCES

(1) Friguet, B.; Chaffotte, A. F.; Djavadiohaniance, L.; Goldberg, M. E. *J. Immunol. Methods* **1985**, *77*, 305.
(2) Owicki, J. C. *J. Biomol. Screening* **2000**, *5*, 297.
(3) Ladbury, J. E.; Chowdhry, B. Z. *Chem. Biol.* **1996**, *3*, 791.
(4) Schuck, P. *Curr. Opin. Biotechnol.* **1997**, *8*, 498.
(5) Pochapsky, S. S.; Pochapsky, T. C. *Curr. Top. Med. Chem.* **2001**, *1*, 427.
(6) Wyss, D. F.; McCoy, M. A.; Senior, M. M. *Curr. Opin. Drug Discovery Dev.* **2002**, *5*, 630.
(7) Lepre, C. A.; Moore, J. M.; Peng, J. W. *Chem. Rev.* **2004**, *104*, 3641.
(8) Connors, K. A. *Binding Constants: The Measurement of Molecular Complex Stability*; Wiley: New York, 1987.
(9) Carlomagno, T. *Annu. Rev. Biophys. Biomed.* **2005**, *34*, 245.
(10) Fielding, L. *Curr. Top. Med. Chem.* **2003**, *3*, 39.
(11) Meyer, B.; Peters, T. *Angew. Chem., Int. Ed.* **2003**, *42*, 864.
(12) Ni, F. *Prog. Nucl. Magn. Reson. Spectrosc.* **1994**, *26*, 517.
(13) Stockman, B. J.; Dalvit, C. *Prog Nucl. Magn. Reson. Spectrosc.* **2002**, *41*, 187.
(14) Carravetta, M.; Levitt, M. H. *J. Am. Chem. Soc.* **2004**, *126*, 6228.
(15) Carravetta, M.; Levitt, M. H. *J. Chem. Phys.* **2005**, *122*, No. 214505.
(16) Levitt, M. H. In *Encyclopedia of Nuclear Magnetic Resonance*; Grant, D. M., Harris, R. K., Eds.; Wiley: Chichester, U.K., 2002; Vol. *9*.
(17) de Bock, C. E.; Wang, Y. *Med. Res. Rev.* **2004**, *24*, 13.
(18) McMahon, B.; Kwaan, H. C. *Pathophysiol. Haemostasis Thromb.* **2008**, *36*, 184.
(19) Mekkawy, A. H.; Morris, D. L.; Pourgholami, M. H. *Future Oncol.* **2009**, *5*, 1487.
(20) Luz, Z.; Meiboom, S. *J. Chem. Phys.* **1964**, *40*, 2686.
(21) McConnell, H. M. *J. Chem. Phys.* **1958**, *28*, 430.
(22) Gopalakrishnan, K.; Bodenhausen, G. *J. Magn. Reson.* **2006**, *182*, 254.
(23) Pileio, G.; Levitt, M. H. *J. Chem. Phys.* **2009**, *130*, No. 214501.
(24) Fejzo, J.; Lepre, C. A.; Peng, J. W.; Bemis, G. W.; Ajay; Murcko, M. A.; Moore, J. M. *Chem. Biol.* **1999**, *6*, 755.
(25) Baishya, B.; Segawa, T. F.; Bodenhausen, G. *J. Am. Chem. Soc.* **2009**, *131*, 17538.
(26) Dalvit, C.; Fagerness, P. E.; Hadden, D. T.; Sarver, R. W.; Stockman, B. J. *J. Am. Chem. Soc.* **2003**, *125*, 7696.
(27) Kronis, K. A.; Carver, J. P. *Biochemistry* **1982**, *21*, 3050.
(28) Aguilar, J. A.; Nilsson, M.; Bodenhausen, G.; Morris, G. A. *Chem. Commun.* **2012**, *48*, 811.
(29) Ahuja, P.; Sarkar, R.; Vasos, P. R.; Bodenhausen, G. *J. Am. Chem. Soc.* **2009**, *131*, 7498.
(30) Heinis, C.; Rutherford, T.; Freund, S.; Winter, G. *Nat. Chem. Biol.* **2009**, *5*, 502.
(31) Ke, S. H.; Coombs, G. S.; Tachias, K.; Corey, D. R.; Madison, E. L. *J. Biol. Chem.* **1997**, *272*, 20456.
(32) Angelini, A.; Cendron, L.; Chen, S.; Touati, J.; Winter, G.; Zanotti, G.; Heinis, C. *ACS Chem. Biol.* **2012**, *7*, 817.
(33) Renatus, M.; Bode, W.; Huber, R.; Sturzebecher, J.; Stubbs, M. T. *J. Med. Chem.* **1998**, *41*, 5445.
(34) Sarkar, R.; Vasos, P. R.; Bodenhausen, G. *J. Am. Chem. Soc.* **2007**, *129*, 328.
(35) Hess, B.; Kutzner, C.; van der Spoel, D.; Lindahl, E. *J. Chem. Theory Comput.* **2008**, *4*, 435.
(36) Oostenbrink, C.; Villa, A.; Mark, A. E.; Van Gunsteren, W. F. *J. Comput. Chem.* **2004**, *25*, 1656.
(37) Kohlhoff, K. J.; Robustelli, P.; Cavalli, A.; Salvatella, X.; Vendruscolo, M. *J. Am. Chem. Soc.* **2009**, *131*, 13894.